Realization of Bose-Einstein Condensates in Lower Dimensions

A. Görlitz,* J. M. Vogels, A. E. Leanhardt, C. Raman, T. L. Gustavson, J. R. Abo-Shaeer, A. P. Chikkatur, S. Gupta, S. Inouye, T. Rosenband, and W. Ketterle

Department of Physics and Research Laboratory of Electronics, Massachusetts Institute of Technology, Cambridge, Massachusetts 02139

(Received 23 April 2001; published 4 September 2001)

Bose-Einstein condensates of sodium atoms have been prepared in optical and magnetic traps in which the energy-level spacing in one or two dimensions exceeds the interaction energy between atoms, realizing condensates of lower dimensionality. The crossover into two-dimensional and one-dimensional condensates was observed by a change in aspect ratio and by the release energy converging to a nonzero value when the number of trapped atoms was reduced.

DOI: 10.1103/PhysRevLett.87.130402 PACS numbers: 03.75.Fi, 34.50.–s, 67.90.+z

The study of one- and two-dimensional systems is an important area in condensed matter physics since the properties of phase transitions and the nature of collective excitations depend on the spatial degrees of freedom. Bose-Einstein condensation (BEC) is impossible in 1D and 2D in a homogenous system, but should occur in atom traps because the confining potential modifies the density of states [1]. In this Letter, we study how condensates in extremely anisotropic traps assume 1D or 2D character when the number of atoms is reduced. Dilute-gas condensates of density n in axially symmetric traps are characterized by four length scales: their radius $R_\perp$, their axial half-length R_z, the scattering length a which parametrizes the strength of the two-body interaction, and the healing length $\xi = (4\pi na)^{-1/2}$ [2]. In almost all experiments on Bose-Einstein condensates, both the radius and length are determined by the interaction between the atoms and, thus, $R_\perp, R_z \gg \xi \gg a$. In this regime, a BEC is three-dimensional and is well described by the so-called Thomas-Fermi approximation [3]. A qualitatively different behavior of a BEC is expected when the healing length is larger than either $R_\perp$ or R_z since then the condensate becomes restricted to one or two dimensions, respectively. Some authors refer to such an energetic restriction as quasi-low-dimensional [4,5]. New phenomena that may be observed in this regime are, for example, quasicondensates with a fluctuating phase [4–6] and a Tonks gas of impenetrable bosons [5,7,8].

In this Letter, we report the experimental realization of cigar-shaped 1D condensates with $R_z > \xi > R_\perp$ and disk-shaped 2D condensates with $R_\perp > \xi > R_z$. The crossover from 3D to 1D or 2D was explored by reducing the number of atoms in condensates which were trapped in highly elongated magnetic traps (1D) and disk-shaped optical traps (2D) and measuring the release energy. In harmonic traps, (quasi)lower dimensionality is reached when $\mu_{3D} = 4\pi\hbar^2 an/m < \hbar\omega_t$. Here ω_t is the trapping frequency in the tightly confining dimension(s) and μ_{3D} is the interaction energy of a weakly interacting BEC, which in 3D corresponds to the chemical potential. Other experiments in which the interaction energy was comparable to the level spacing of the confining potential include condensates in one-dimensional [9] and recently two-dimensional [10] optical lattices and the crossover to an ideal-gas (zero-D) condensate [11], all at relatively low numbers of condensate atoms.

Naturally, the number of interacting atoms in (quasi)low-dimensional condensates is limited. The peak interaction energy of a 3D condensate of N atoms with mass m is given by $\mu_{3D} = \hbar^2/2m(15Na/l_z^2 l_\perp^4)^{2/5}$, where $l_{\perp,z} = (\hbar/m\omega_{\perp,z})^{1/2}$ are the oscillator lengths of the harmonic potential. The crossover to 1D and 2D, defined by $\mu_{3D} = \hbar\omega_t$ or equivalently $\xi = l_t$, occurs if the number of condensate atoms becomes

$$N_{1D} = \sqrt{\frac{32\hbar}{225ma^2}}\sqrt{\frac{\omega_\perp}{\omega_z^2}} = \sqrt{\frac{\omega_\perp}{\omega_z^2}} \times 7100 \left(\frac{\text{rad}}{\text{s}}\right)^{1/2}, \quad (1)$$

$$N_{2D} = \sqrt{\frac{32\hbar}{225ma^2}}\sqrt{\frac{\omega_z^3}{\omega_\perp^4}} = \sqrt{\frac{\omega_z^3}{\omega_\perp^4}} \times 7100 \left(\frac{\text{rad}}{\text{s}}\right)^{1/2}, \quad (2)$$

where we have used the scattering length ($a = 2.80$ nm [12]) and mass of ^{23}Na atoms to derive the numerical factor. Our traps feature extreme aspect ratios resulting in $N_{1D} > 10^4$ and $N_{2D} > 10^5$, while for most standard BEC traps the numbers are significantly smaller.

For the 1D case, the condition $\xi = l_t$ yields a linear density $\tilde{n}_{1D} \approx 1/4a$, implying that the linear density of a 1D condensate is limited to less than one atom per scattering length independent of the radial confinement. Therefore, tight transverse confinement, as may be achievable in small magnetic waveguides [13] or hollow laser beam guides [14], is by itself not helpful to increase the number of atoms in a 1D condensate. Large 1D numbers may be achieved only at the expense of longer condensates or if the scattering length is smaller.

In anisotropic traps, a primary indicator of crossing the transition temperature for Bose-Einstein condensation is

a sudden change of the aspect ratio of the ballistically expanding cloud, and an abrupt change in its energy. The transition to lower dimensions is a smooth crossover, but has similar indicators. In the 3D Thomas-Fermi limit, the degree of anisotropy of a BEC is independent of the number N of atoms, whereas in 1D and 2D, the aspect ratio depends on N. Similarly, the release energy in 3D depends on N [3] while in lower dimensions, it saturates at the zero-point energy of the tightly confining dimension(s).

A trapped 3D condensate has a parabolic shape, and its radius and half-length are given by $R_\perp = l_\perp(15Nal_\perp/l_z^2)^{1/5}$ and $R_z = l_z(15Nal_z^3/l_\perp^4)^{1/5}$ [3], resulting in an aspect ratio of $R_\perp/R_z = l_\perp^2/l_z^2 = \omega_z/\omega_\perp$. When the 2D regime is approached by reducing the atom number, the condensate assumes a Gaussian shape with an rms width $\approx l_z$ along the axial direction, but retains the parabolic shape radially. The radius of a trapped 2D condensate decreases with N as $R_\perp = (128/\pi)^{1/8}(Nal_\perp^4/l_z)^{1/4}$ [4]. Similarly, the half-length of trapped 1D condensates is $R_z = (3Nal_z^4/l_\perp^2)^{1/3}$ [5].

Our experiments in which 1D and 2D BECs were realized were carried out in two different experimental setups. For the study of condensates in a 2D geometry, condensates of $\approx 10^7$ atoms were generated as described in Refs. [15,16] and transferred into an optical trap [17]. The optical trapping potential was generated by focusing a 1064 nm laser into a light sheet using cylindrical lenses, with the tight focus in the vertical dimension to provide optimum support against gravity. This resulted in typical trap frequencies of $\omega_z/2\pi = 790$ Hz, $\omega_{\perp x}/2\pi = 30$ Hz, and $\omega_{\perp y}/2\pi = 10$ Hz for a laser power of $\approx$500 mW. The axial level spacing in this trap corresponds to a temperature of $T = \hbar\omega_z/k_B \approx 40$ nK, and the axial harmonic oscillator length was $l_z = 0.75$ μm. The transfer from the magnetic trap into the optical trap was accomplished by turning on the trapping light field and turning down the magnetic trapping potential resulting in a transfer efficiency of more than 50%. The depth of the optical potential and the trap frequencies could be easily varied by changing the power of the trapping beam.

To observe the transition from the 3D Thomas-Fermi regime into a 2D situation, we have adjusted the number of condensate atoms between 2×10^6 and 2×10^4 by exposing the optically trapped BEC to a thermal sodium atomic beam. Condensates were detected by suddenly releasing the atoms from the trap and taking absorption images after 15 ms free expansion. The condensates dropped by 15 μm during the 100 μs imaging time, which is not more than 10% of the measured length of our shortest condensates. During expansion, the interaction energy is converted almost exclusively into kinetic energy in the tightly confining vertical dimension. Thus, the horizontal radius of the condensate remains almost unchanged while the vertical length expands quickly, and after 15 ms the length is even larger than the radius. Length and radius were determined by fitting the condensate with a parabolic Thomas-Fermi distribution which is exact in the large-number limit. For small numbers, the vertical condensate shape approaches a Gaussian, but we also used the parabolic fitting function to avoid any bias. A parabolic fitting function may underestimate the rms width of a Gaussian by at most 20%.

Figures 1a and 1b show how the expanded condensate became more elongated for small atom numbers, clear evidence for approaching 2D. In Fig. 1c the aspect ratio of condensates in three different optical traps is shown. In all three traps, the aspect ratio approaches a constant value for large atom numbers, which can be calculated using the results of [18] for the Thomas-Fermi limit. The increase of the aspect ratio for small atom numbers is due to clamping of the vertical length of the condensate because of saturation of the release energy while the width shrinks further. For the weakest trap, using Eq. (2), $N_{2D} = 2.9 \times 10^5$, while we could observe condensates with atom numbers lower than $N_{2D}/10$.

The saturation of the mean release energy per particle at the kinetic part of the zero-point energy of the trap becomes obvious if the half-length of the expanded condensates is plotted versus the radius (see Fig. 2). For a long enough time of flight, the mean release energy is simply

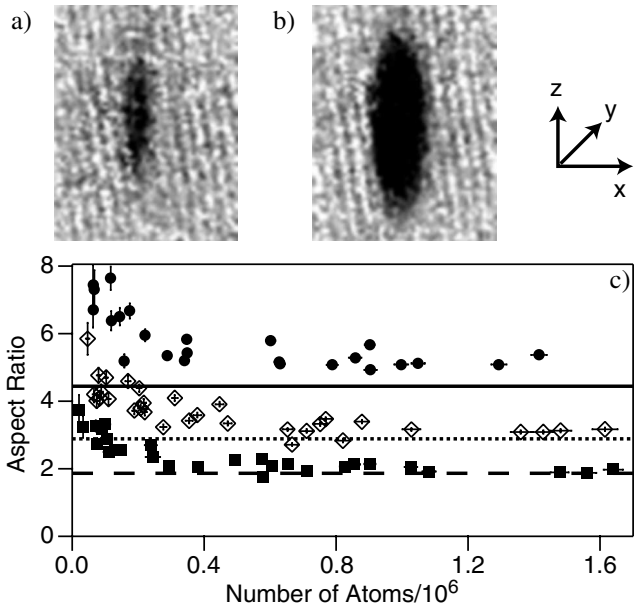

FIG. 1. Crossover from 3D to 2D, observed in the change of the aspect ratio after 15 ms time of flight. (a) A 2D condensate with 8×10^4 atoms. (b) A 3D condensate with 7×10^5 atoms in a trap with vertical trap frequency of $\omega_z/2\pi \approx 790$ Hz. (c) Aspect ratio as a function of atom number for optical traps with $\omega_z/2\pi \approx 1620$ Hz (filled circles), 790 Hz (open diamonds), and 450 Hz (filled squares). The lines indicate the aspect ratios as expected for 3D condensates. We attribute discrepancies between expected and measured aspect ratios for large numbers to the influence of anharmonicities on the measurement of the trap frequencies. Where given, the error bars represent only the error from fitting of the condensate shape.

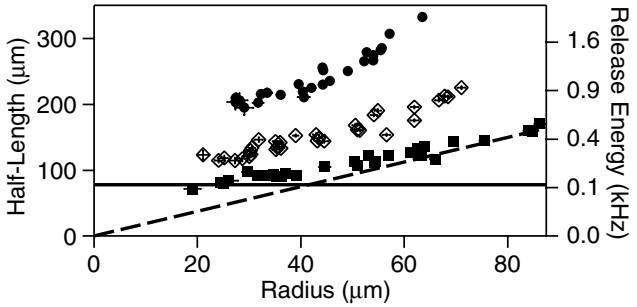

FIG. 2. Half-length and release energy versus radius for the same optical traps as in Fig. 1. As the condensates cross over from 3D to 2D the half length approaches a constant value. The dashed line represents the expected behavior of a purely 3D condensate and the solid line the expected 2D saturation level of the release energy for the weakest trap (filled squares).

proportional to the square of the measured half-length and is given by $E_{\mathrm{rel}} = mR_z(t)^2/14t^2$. In all our traps the half-length appears to approach a constant value corresponding to a release energy close to $\hbar\omega_z/4$, the vertical kinetic zero-point energy.

The 1D experiments were carried out in a Ioffe-Pritchard–type magnetic trap with radial and axial trapping frequencies of $\omega_\perp/2\pi = 360$ Hz and $\omega_z/2\pi = 3.5$ Hz [19]. We obtained an extreme aspect ratio of $\sim$100 by reducing the axial confinement during the final evaporation stage. As in the 2D case, the number of atoms in the condensate was lowered by exposing the gas to a thermal sodium beam, followed by a reequilibration time of 15 s. A radiofrequency shield [16] limited the trap depth to 10–40 kHz (0.5–2 μK). This ensured condensate fractions of at least 50%. We analyzed the cloud using absorption imaging along one of the radial directions after a ballistic expansion of $t = 4$ ms. In contrast to the 2D experiments, the aspect ratio of the cloud was not yet inverted after this short time of flight. The measured condensate sizes were corrected for the finite imaging resolution of 5 μm, a correction of less than 10%.

Similar to the 2D experiment, the crossover to 1D was observed by a change of the aspect ratio when the number of atoms was reduced (Fig. 3). In the 3D limit, neglecting the initial radial size and the axial expansion (both $<1\%$ corrections) the aspect ratio equals $\omega_z t$ independent of N. The deviation from this behavior below $\approx 5 \times 10^4$ atoms demonstrates the crossover to 1D. At the same time, the release energy approached $\hbar\omega_\perp/2$, the zero-point kinetic energy of the trapping potential (Fig. 3b). For this trap, Eq. (1) yields $N_{1\mathrm{D}} = 1.5 \times 10^4$, while we could observe condensates with N as low as $N_{1\mathrm{D}}/2$. Note that at the crossover to 2D the interaction energy per particle is roughly equal to the kinetic zero-point energy, while at the crossover to 1D it is only approximately half the kinetic zero-point energy. Thus, in the 1D geometry, the aspect ratio deviates from the 3D limit for larger ratios of $N/N_{1\mathrm{D}}$ than in the 2D case.

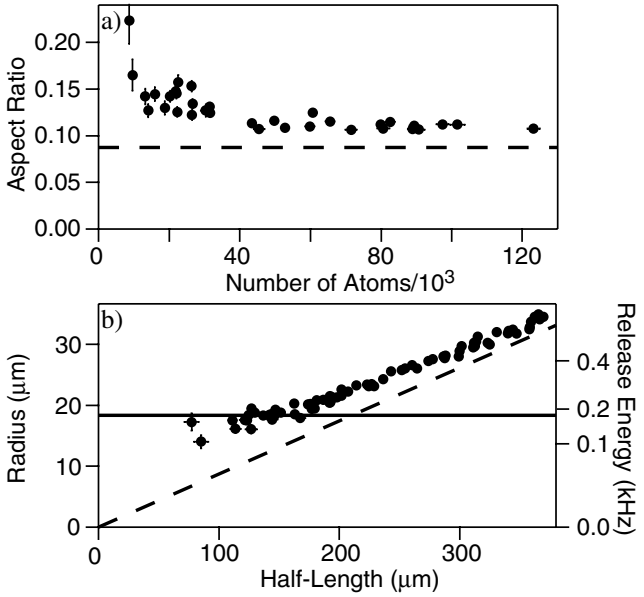

FIG. 3. Crossover from 3D to 1D. (a) Aspect ratio after 4 ms time of flight versus atom number. (b) Radius versus half-length for the same data. The release energy approaches the expected constant value (solid line) for low atom number. The dashed line represents the behavior of a 3D condensate. Note that the use of a parabolic fitting function slightly underestimates the release energy in the 1D regime.

So far, we have discussed only the condensate and its crossover from the 3D to a (quasi)lower-dimensional situation. Here we will briefly address the thermal component and finite temperature effects. The finite trap depth provides constant evaporative cooling which counteracts any residual heating and stabilizes the temperature at a constant fraction $1/\eta$ of the trap depth U_{trap}. For a quantum saturated thermal cloud ($T < T_c$), the number of thermal atoms N_{th} can be approximated by simply counting the number of states with an energy below $k_B T$, which results in $N_{\mathrm{th}} \approx (U_{\mathrm{trap}}/\eta\hbar)^3/\omega_\perp^2\omega_z$. This estimate assumes that the thermal cloud is still three dimensional ($k_B T > \hbar\omega_{\perp,z}$), in agreement with the situation in the experiment. To be able to discern the condensate from the thermal cloud, N_{th} should not be much larger than $N_{1\mathrm{D}}$ ($N_{2\mathrm{D}}$). This simple argument implies that for our 1D trap where $N_{1\mathrm{D}} \approx 1.5 \times 10^4$, the maximum allowed trap depth would be 40 kHz assuming a typical $\eta = 10$ and a minimum condensate fraction of 10%. This is in fair agreement with our experimental observations.

In a magnetic trap, the trap depth can be adjusted independently of the trap frequencies using an rf shield. In an optical trap created using a single Gaussian focus, the trap frequencies are proportional to the square root of the trap depth. Thus, tighter optical traps can store more thermal atoms, yet Eq. (2) implies that $N_{2\mathrm{D}}$ is lower for tighter traps. Therefore, tight single-focus optical traps are less suitable for the observation of lower-dimensional condensates. Experimentally, we have observed that for weaker

traps we could penetrate further into the 2D regime (see Fig. 1c) than for tighter ones, which is consistent with the considerations above.

In our experiments, the thermal cloud is always three-dimensional, implying that the critical temperature T_c for Bose condensation is also larger than the energy-level spacing of the trap, i.e., $k_B T_c > k_B T > \hbar\omega_t$. A new physical regime in which the condensation process could be studied in lower dimensions would be reached if thermal excitations freeze out before a BEC forms. This requires that the total number of atoms N be smaller than the number of states with an energy smaller than $\hbar\omega_t$. Thus, in 1D, the number of atoms may not exceed the aspect ratio of the trap, i.e., $N < A = \omega_t/\omega_w$, where ω_w is the trapping frequency in the weakly confining direction, while in 2D the relevant criterion is $N < A^2$. For the traps used in our experiments, this implies $N < 100$ (1D) or $N < 2500$ (2D), which, at least for 2D, seems to be within experimental reach. It is not yet clear under what circumstances one will observe quasicondensates [4,6] or the Kosterlitz-Thouless transition [20]. A full understanding of the observation of 2D quantum degeneracy of spin-polarized hydrogen [21] is still lacking, and controlled experiments with dilute gases could give useful insights. In a 1D geometry, a related effect that could be observed is a two-step condensation as discussed in [22].

Lower-dimensional condensates, as prepared in our experiments, offer many opportunities for further scientific studies. Topological excitations such as solitons (in 1D) and vortices (in 2D) should be much more stable than in 3D, where solitons suffer from kink instabilities and vortices can bend. The character and spectrum of the collective excitations is expected to exhibit a qualitative change in lower dimensions [23].

Another area of significant interest is the study of quasicondensates [4–6], which locally behave like ordinary condensates but do not have a globally uniform phase. Such phase fluctuations have recently been observed in 3D [24]. However, the importance of phase fluctuations is expected to be more pronounced in lower dimensions.

An even more ambitious goal is the observation of a Tonks gas in a one-dimensional geometry [5,7,8]. At zero temperature, such a gas of "impenetrable bosons" is realized when the axial distance $1/\tilde{n}$ between atoms exceeds the 1D healing length, $\xi = l_\perp/(2\tilde{n}a)^{1/2}$ [5], resulting in $\tilde{n}_{\mathrm{Tonks}} = 2a/l_\perp^2$ as a condition for the linear density. Thus, $\tilde{n}_{\mathrm{Tonks}}$ is $8a^2/l_\perp^2$ times smaller than $\tilde{n}_{1\mathrm{D}}$. In 2D, the collision physics is severely altered only for $a/R_z > 1$ [4]. Such regimes require much tighter confinement than in our experiment and may be realized using optical lattices or magnetic microtraps, or alternatively a larger scattering length, e.g., near a Feshbach resonance.

In conclusion, we have prepared (quasi-)low-dimensional condensates in optical and magnetic traps. Because of the extreme geometries of our traps, the number of atoms at the crossover is rather large ($>10^5$ in the 2D case) which provides a good starting point for the exploration of phenomena which occur only in one or two dimensions.

This research is supported by NSF, ONR, ARO, NASA, and the David and Lucile Packard Foundation. A. G., A. E. L., and A. P. C. acknowledge additional support from DAAD, NSF, and JSEP, respectively.

Note added.—Very recently, (quasi)1D condensates in a magnetic trap were also realized with lithium [25].

*Current address: Universität Stuttgart, 5 Phys. Inst., Germany.

[1] V. Bagnato and D. Kleppner, Phys. Rev. A **44**, 7439 (1991).
[2] Here the healing length is defined as $\xi = (\hbar^2/m\mu)^{1/2}$ as in [4,5], whereas [3] uses $\xi = (\hbar^2/2m\mu)^{1/2}$.
[3] F. Dalfovo *et al.,* Rev. Mod. Phys. **71**, 463 (1999).
[4] D. S. Petrov, M. Holzmann, and G. V. Shlyapnikov, Phys. Rev. Lett. **84**, 2551 (2000).
[5] D. S. Petrov, G. V. Shlyapnikov, and J. T. M. Walraven, Phys. Rev. Lett. **85**, 3745 (2000).
[6] Y. Kagan, B. V. Svistunov, and G. V. Shlyapnikov, Sov. Phys. JETP **66**, 314 (1987).
[7] L. Tonks, Phys. Rev. **50**, 955 (1936).
[8] M. Olshanii, Phys. Rev. Lett. **81**, 938 (1998).
[9] C. Orzel *et al.,* Science **291**, 2386 (2001).
[10] M. Greiner *et al.,* cond-mat/0105105.
[11] M. Holland *et al.,* Phys. Rev. Lett. **78**, 3801 (1997).
[12] C. Samuelis *et al.,* Phys. Rev. A **63**, 012710 (2000).
[13] J. Fortagh *et al.,* Phys. Rev. Lett. **81**, 5310 (1998); J. Reichel, W. Hänsel, and T. W. Hänsch, *ibid.* **83**, 3398 (1999); D. Müller *et al., ibid.* **83**, 5194 (1999); N. H. Dekker *et al., ibid.* **84**, 1124 (2000); M. Key *et al., ibid.* **84**, 1371 (2000); R. Folman *et al., ibid.* **84**, 4749 (2000).
[14] T. Kuga *et al.,* Phys. Rev. Lett. **78**, 4713 (1997); K. Bongs *et al.,* Phys. Rev. A **63**, 031602(R) (2001).
[15] M. O. Mewes *et al.,* Phys. Rev. Lett. **77**, 416 (1996).
[16] W. Ketterle, D. S. Durfee, and D. M. Stamper-Kurn, in *Bose-Einstein Condensation in Atomic Gases,* Proceedings of the International School of Physics "Enrico Fermi," Course CXL, edited by M. Inguscio, S. Stringari, and C. Wieman (IOS Press, Amsterdam, 1999), p. 67.
[17] D. M. Stamper-Kurn *et al.,* Phys. Rev. Lett. **80**, 2027 (1998).
[18] Y. Castin and R. Dum, Phys. Rev. Lett. **77**, 5315 (1996).
[19] R. Onofrio *et al.,* Phys. Rev. Lett. **84**, 810 (2000).
[20] W. J. Mullin, M. Holzmann, and F. Laloë, J. Low Temp. Phys. **121**, 263 (2000).
[21] A. I. Safonov *et al.,* Phys. Rev. Lett. **81**, 4545 (1998).
[22] N. J. van Druten and W. Ketterle, Phys. Rev. Lett. **79**, 549 (1997).
[23] T. L. Ho and M. Ma, J. Low Temp. Phys. **115**, 61 (1999); S. Stringari, Phys. Rev. A **58**, 2385 (1998).
[24] D. S. Petrov, G. V. Shlyapnikov, and J. T. M. Walraven, Phys. Rev. Lett. **87**, 050404 (2001); S. Dettmer *et al.,* cond-mat/0105525.
[25] F. Schreck *et al.,* Phys. Rev. Lett. **87**, 080403 (2001).